PAPER

Compensation of Transmitter Memory Nonlinearity by Post-Reception Blind Nonlinear Compensator with FDE

Yasushi YAMAO[†a)], ***Fellow***, **Tetsuki TANIGUCHI**[†], ***Member***, ***and*** **Hiroki ITO**[†], ***Student Member***

SUMMARY High-accuracy wideband signal transmission is essential for 5G and Beyond wireless communication systems. Memory nonlinearity in transmitters is a serious issue for the goal, because it deteriorates the quality of signal and lowers the system performance. This paper studies a post-reception nonlinear compensation (PRC) schemes consisting of frequency domain equalizers (FDEs) and a blind nonlinear compensator (BNLC). A frequency-domain memory nonlinearity modeling approach is employed, and several PRC configurations with FDEs and BNLC are evaluated through computer simulations. It is concluded that the proposed PRC schemes can effectively compensate memory nonlinearity in wideband transmitters via frequency-selective propagation channel. By implementing the PRC in a base station, uplink performance will be enhanced without any additional cost and power consumption in user terminals.

key words: *5G, nonlinear compensation, memory effect, BNLC, EVM*

1. Introduction

Developments of enhanced 5G and its beyond system have been conducted globally. The use of wider radio-frequency (RF) signal bandwidth is becoming common by employing higher frequency bands such as millimeter wave and Terahertz [1], [2]. At the same time, studies to improve spectrum efficiency by enhancing the signal multiplexing and employing higher modulation index are continued. Non-orthogonal multiple access (NOMA) [3] and higher-level QAM modulation are examples of the research items. These signaling schemes require high-accuracy linear transmission to obtain expected performances.

However, nonlinearity in RF circuits including power amplifiers and mixers affects linear transmission in wireless systems. Particularly, complex nonlinearity with memory effect (hereafter we call it "memory nonlinearity") often appears in wideband RF amplifiers [4] and severely degrades signal quality. Therefore, it is necessary to find an efficient nonlinear compensation technique against memory nonlinearity and realize highly-accurate linear transmission throughout transmitter (Tx) and receiver (Rx).

In addition, high-throughput uplink transmission is essential to realize "digital twin", in which real-world information is uploaded to the virtual world for reconstructing the real world on it [5]. In order to realize the concept, user terminals (UEs) should be able to transmit huge amount of information to the network. However, it is a difficult task for the UEs with limited power source and cost reduction requirement. For instance, 256 QAM gives the highest throughput in 5G uplink when UE can satisfy the Tx error vector magnitude (EVM) requirement of less than 3.5 % [6]. However, a considerable Tx backoff is necessary to achieve this value without accurate nonlinear compensation, which results in reducing the available output power and losing chance of 256 QAM transmission.

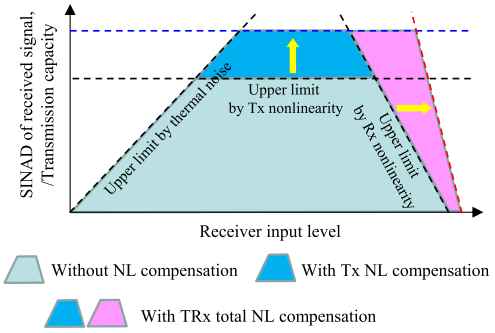

Fig. 1 Transmission capacity limitation of radio communication system suffering from thermal noise and nonlinear (NL) distortions.

In general, basic capacity of wireless transmission, or "channel capacity without interference", is determined by the signal to noise and distortion ratio (SINAD) at Rx input. The effect of nonlinear distortion on a wireless transmission system is illustrated in Fig. 1 as the function of Rx input level. Nonlinear distortion may occur in either Tx or Rx or the both, and its effect to reduce transmission capacity differs depending on the Rx input level. When the input level is small, thermal noise is the major cause of capacity reduction and the effect of nonlinear distortion is not obvious. Since Tx nonlinearity degrades the EVM of transmitted signal, it determines upper limit of the capacity by restricting the selection of higher-level modulation schemes. On the other hand, the nonlinearity effect caused by Rx saturation depends on the input power including other RF signals in adjacent frequency bands. From the figure, it is understood that introducing an effective nonlinear compensation scheme throughout Tx and Rx is very important to enhance transmission capacity.

Nonlinear compensation techniques are categorized into two concepts, Tx compensation and post-reception compensation (PRC). Tx compensation schemes have been widely applied for mobile communication base station

Manuscript received September 5, 2022.
Manuscript revised November 30, 2022.
Manuscript publicized January 11, 2023.
[†]The authors are with Advanced Wireless Communication & Research Center, The University of Electro-Communications, Chofu-shi, 182-8585 Japan.
a) E-mail: yyamao@m.ieice.org
DOI: 10.1587/transcom.2022EBT0004

transmitters. The most common technique is a digital predistortion (DPD) [7]. It can reduce adjacent channel radiation power that is strictly regulated in UHF and Sub-6 GHz bands. However, nonlinear compensation by Tx alone cannot achieve linear transmission throughout Tx and Rx.

PRC [8] has been developed to solve the issue of Rx nonlinearity. The blind nonlinear compensator (BNLC) [9]–[15] is one of the most promising PRC technique that can be realized in digital signal processing domain without requiring any RF circuits. Its performance against Rx nonlinearity was examined under flat Rayleigh fading propagation environments [12]. It does not require additional signal information to determine the compensator coefficients, apart from the bandwidth and center frequency. Therefore, BNLC can be widely applied to many systems because it is independent from modulation schemes and signal formats.

Moreover, recent studies [13], [14] reveal the potential of BNLC to compensate not only Rx nonlinearity but also Tx nonlinearity via radio channel. This will make uplink nonlinear compensation feasible by implementing BNLC-based PRC in a base station, without any additional cost and power consumption in user terminals. By introducing the PRC, uplink signal quality can be improved without large Tx backoff in user terminals. Thus uplink throughput will be enhanced by employing high-level modulation with sufficient output power. Therefore, BNLC-based PRC will be a promising solution to realize highly-accurate linear transmission throughout Tx and Rx and enhance the system capacity. However, the previous works [13], [14] did not consider complex nonlinearity with memory effects.

The basic study of memory-nonlinearity compensation by BNLC-based PRC was done in [15], not including the effect of radio propagation channel with fading and additive thermal noise. Then the question remains that the PRC can still compensate Tx memory effect via frequency-selective fading channel. It is identified as a complex problem that frequency-selective linear distortions are combined with nonlinear distortion. Since linear and nonlinear distortions affect each other, they cannot be treated independently in time domain. Another concern is the effect of additive thermal noise, which may affects PRC performance.

Therefore, this paper pursues BNLC-based PRC that can compensate Tx memory nonlinearity through frequency-selective fading channel with thermal noise. We first focus on the memory nonlinearity modeling methods, finding that frequency-domain nonlinear modeling and compensation are effective for realizing PRC via fading channel. In the frequency-domain processing, Tx memory effect and fading channel can be equalized by frequency-domain equalizers (FDEs). Several configurations of PRC with BNLC and FDE are proposed and their performances are evaluated under the propagation channel.

The remainder of this paper is organized as follows. In Sect. 2, we review nonlinear models with memory effect and compare time-domain and frequency-domain modeling. After giving the basic information of BNLC and FDE in Sect. 3, we propose PRC configurations with BNLC and FDE in Sect. 4. The performance of the proposed PRCs are evaluated in Sect. 5 by computer simulations. The conclusions of the study are presented in Sect. 6.

2. Nonlinear Model with Memory Effect

In nonlinear compensation, an input-output characteristic is identified first, then it is translated to a mathematical model. By obtaining the inverse function of the model, compensation is conducted. The mathematical model has a strong impact on the compensation performance.

2.1 Memory Effect and Its Modeling Method

RF circuits using active devices such as amplifiers and mixers present output saturation. Moreover, the saturation power and linear gain often present frequency dependency as shown in Fig. 2. Such characteristics are attributed to the reactive elements of device and matching circuits, as well as the device temperature change due to the dynamic variation of input signal amplitude [4]. A circuit with such frequency characteristic has a certain length of impulse response, which causes memory effect in nonlinearity. To express memory nonlinearity, many nonlinear models have been proposed [7]. Most of them base on the time-domain nonlinear model without memory effect (hereafter we call it "memoryless nonlinear model (ML-NLM)", adding memory-effects either in time-domain or frequency-domain. As the ML-NLM, a polynomial model is commonly used.

In the time-domain memory approaches, the most fundamental method is Volterra-series model [7]. In the model, memory effects are expressed by the multidimensional convolutions of linear and nonlinear output signal samples. Nonlinear output signal samples generated by the ML-NLM are delayed and overlapped to the signal according to the impulse response. This process is repeated because the convolution results also suffer from nonlinearity. Supposing discrete-time equivalent baseband signal processing, nonlinear output is obtained from higher-dimensional convolution space, which requires huge amount of calculation when the impulse response is long. In order to reduce the complexity of calculation to a practical level, simplified models have been developed, such as memory polynomial [16] and generalized memory polynomial [17]. However, there is a

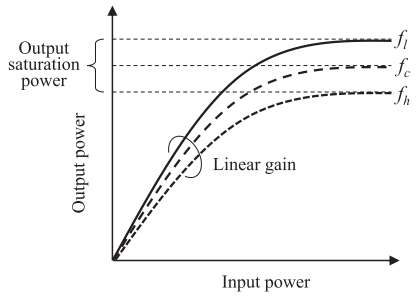

Fig. 2 Example of frequency-dependent nonlinear characteristic.

trade-off between calculation reduction and compensation accuracy [17]. To obtain better performance, more complicated models are needed.

In frequency-domain memory approaches, nonlinear signals are converted from time-domain to frequency-domain by discrete Fourier transform (DFT) and its inverse method (IDFT). A memory effect is added by multiplying the filtering transfer function corresponding to the impulse response. Thus, convolution is not necessary and the amount of calculation can be reduced [15]. Moreover, frequency-domain processing has commonality with recent wideband modulation schemes including Orthogonal Frequency Division Multiplexing (OFDM) and Single Carrier Frequency Division Multiple Access (SC-FDMA). Therefore, we focus on the frequency-domain memory modeling approach in equivalent baseband.

2.2 Frequency-Domain Memory Nonlinear Model

Well-known frequency-domain memory nonlinear models are as follows [7], [18].

a) Wiener model
b) Hammerstein model
c) Wiener-Hammerstein model

Figure 3 shows block diagrams of the above models. They include ML-NLM and cascaded memory-effect filters. Since ML-NLM is a time-domain polynomial model, DFT and IDFT blocks are necessary at the input and output of ML-NLM in the actual implementation. These blocks are omitted in the figure for simplification. The position of memory-effect filters is either before or after the ML-NLM, or the both. Supposing an amplifier, the filters represent memory effects caused by reactive components of the device input or output ports and matching circuits before or after the device. In this sense, Wiener-Hammerstein model is the most general model. Hereafter we employ it as the default model. In order to identify a frequency-domain memory nonlinear model, the coefficients of ML-NLM polynomial and the transfer function of the memory-effect filters should be determined. To express the memory-effect due to temperature change in the device, modifications with additional filters have been proposed that consider internal thermal accumulation and diffusion [19].

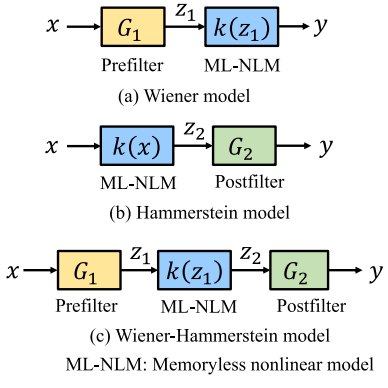

Fig. 3 Frequency-domain memory nonlinear models.

3. PRC Components

According to the frequency-domain memory nonlinear modeling approach, we choose BNLC and FDEs as the essential components for configuring PRC. In the approach, memory effects and frequency-selective fading channel are equalized by FDEs and their effects are removed. Nonlinearity after removing the frequency dependency is compensated by the BNLC with a memoryless compensator.

3.1 BNLC

Figure 4 shows the block diagram of the BNLC [14]. It is assumed that the transmitted signal is unknown and the only information available is bandwidth and center frequency of the signal. For the ML-NLM, a simple polynomial model is employed in which an RF circuit nonlinearity is expressed as an equivalent baseband polynomial [20]:

$$y = \sum_{\substack{p=1 \\ \text{odd}}}^{P} a_p |x|^{p-1} x \tag{1}$$

where x and y are the input and output signals of a nonlinear circuit in the continuous-time domain, respectively. P is the maximum order of nonlinearity, a_p is the p_{th} order nonlinear coefficient. Here, x, y, and a_p are complex numbers in equivalent baseband.

After the nonlinear output y is input to the BNLC, the similar polynomial form can be used in the BNLC nonlinear compensator to realize an inverse characteristic of the nonlinear circuit. The input/output characteristics of the memoryless compensator are given by:

$$z = \sum_{\substack{q=1 \\ \text{odd}}}^{Q} b_q |y|^{q-1} y \tag{2}$$

where y and z are the input and output signals of the compensator in the continuous-time domain, respectively. Q is the maximum order of nonlinear compensation, and b_q is the q_{th} order compensator coefficient. Q must be equal to or higher than P to achieve high-accuracy compensation.

Nonlinear distortions generated in RF circuit devices

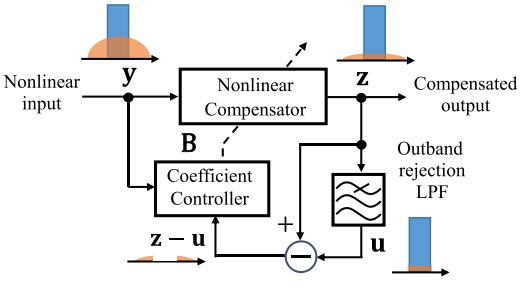

Fig. 4 Block diagram of BNLC.

have strong correlation between the in-band and outband components in frequency spectrum. By using this property, BNLC determines the coefficient b_q that can minimize the nonlinear distortion power. In discrete-time digital signal processing, y, z, and u are replaced by sample vectors with L samples in a unit processing block. Eq. (2) can be expressed in the discrete-time domain as:

$$\mathbf{z} = \mathbf{K}_Q(\mathbf{y})\mathbf{B} \tag{3}$$

$$\mathbf{K}_Q(\mathbf{y}) = \begin{bmatrix} y_1 & |y_1|^2 y_1 & \cdots & |y_1|^{Q-1} y_1 \\ y_2 & |y_2|^2 y_2 & & |y_2|^{Q-1} y_2 \\ \vdots & \vdots & \ddots & \vdots \\ y_L & |y_L|^2 y_L & \cdots & |y_L|^{Q-1} y_L \end{bmatrix} \tag{4}$$

$$\mathbf{B} = \left[b_1, b_3, \ldots, b_q, \ldots, b_Q\right]^{\mathrm{T}} \tag{5}$$

where $\mathbf{K}_Q(\mathbf{y})$ is the kernel matrix of the inverse characteristic polynomial of $L \times (Q+1)/2$. $\mathbf{B}$ is the compensator coefficient vector. From the equations defined above, the outband signal power can be represented as:

$$\begin{aligned} P_{\text{out}} &= \sum_{l=1}^{L} |z_l - u_l|^2 \\ &= \|\mathbf{z} - \mathbf{u}\|^2 \\ &= \left\|\mathbf{K}_Q(\mathbf{y})\mathbf{B} - \mathbf{u}\right\|^2 \end{aligned} \tag{6}$$

where u_l is a time-series sample output from the outband rejection lowpass filter shown in Fig. 4. $\mathbf{B}$ can be determined to minimize the outband signal power using the least square (LS) method and can be defined as:

$$\mathbf{B} = \left(\mathbf{K}_Q^{\mathrm{H}}(\mathbf{y})\mathbf{K}_Q(\mathbf{y})\right)^{-1} \mathbf{K}_Q^{\mathrm{H}}(\mathbf{y})\mathbf{u}. \tag{7}$$

3.2 FDE

FDE can be easily realized in frequency-domain by multiplying a transfer function that cancels the frequency response of a circuit or channel. Many studies on FDEs have been done to remove the effect of frequency-selective fading in mobile communications [21]–[23]. They show that reception performance with FDE greatly depends on the transfer function. Typical algorithms for obtaining the transfer function are Zero-Forcing (ZF) and Minimum Mean Square Error (MMSE) methods.

ZF-FDE multiplies the exact inverse transfer function of a circuit or channel,

$$\boldsymbol{Y}(f) = \boldsymbol{G}(f)^{-1}\boldsymbol{X}(f) \tag{8}$$

where $\boldsymbol{X}$ and $\boldsymbol{Y}$ are the input and output signals of the FDE in frequency domain. $\boldsymbol{G}$ is the transfer function of the circuit or channel, which is normalized in amplitude so that it gives the unity power gain. If the transmitted signal is an LTE-A or 5G-like signal, pilot signals are inserted at several sub-carrier intervals and Rx can estimate channel transfer function $\boldsymbol{G}$ with them.

Although ZF-FDE can fully compensate the frequency response, noise enhancement is a big issue if the circuit or channel has null or deep attenuation points in their frequency responses. It deteriorates reception performance when reception SNR is low. To mitigate the performance degradation under noisy environments, Minimum Mean Square Error (MMSE) FDE is used [22]. The relation of the input and output signals for MMSE-FDE is given by

$$\boldsymbol{Y}(f) = \boldsymbol{W}(f)\boldsymbol{X}(f) \tag{9}$$

$$\boldsymbol{W}(f) = \frac{\boldsymbol{G}^*(f)}{\boldsymbol{G}(f)\boldsymbol{G}^*(f) + 1/SNR}. \tag{10}$$

4. Compensation of Compound Distortion Using FDE and BNLC

4.1 Simultaneous Equalization of Frequency-Selective Channel and Memory Effect

The effect of fading channel appears in both time and frequency domains. It was shown that BNLC has tolerance for flat Rayleigh fading by choosing a suitable sample block size in time-domain signal processing [14]. On the other hand, frequency-selective channel can be treated as a linear filter with a delay spread that causes waveform distortion on the signal. Then the signal processing block diagram of frequency-domain PRC can be illustrated as in Fig. 5. For the memoryless Tx nonlinearity case in (a), a channel transfer function H can be equalized by FDE before BNLC.

For the case of Tx nonlinearity with a Wiener-Hammerstein memory effect, additional FDEs that have the inverse transfer functions of pre- and post-filters, G_1, G_2, should be placed after and before BNLC. Then, FDE for equalizing G_2 can be combined with the channel FDE and the integrated FDE having transfer functions of $(HG_2)^{-1}$ is placed before BNLC as shown in Fig. 5(b). Consequently, BNLC is interposed between two FDEs. We call this configuration "tandem FDE". With the tandem FDE PRC configuration, all linear distortions caused by memory effect and fading channel are equalized by FDEs and the role of BNLC is to compensate pure memoryless nonlinearity. Thus, the compound distortion can be decomposed into linear distortion and memoryless nonlinear distortion.

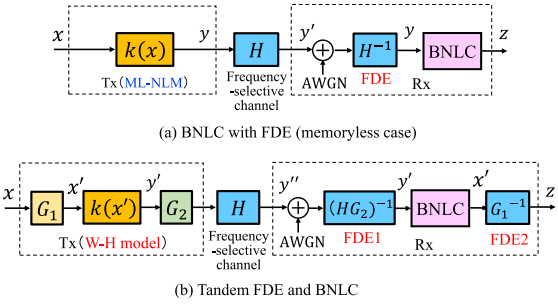

(a) BNLC with FDE (memoryless case)

(b) Tandem FDE and BNLC

Fig. 5 Block diagram of frequency-domain PRC.

4.2 PRCs with Unified FDE and Tx Pre-Equalizer

Although the PRC with tandem FDE configuration enables the ideal decomposition of compound distortion, an important condition should be satisfied that Rx can separate the transfer functions of pre- and post-filters, G_1 and G_2. However, this condition is difficult to satisfy when Rx has little information on the Tx. In the actual systems, Rx may receive signals from many different Txs that have different G_1, G_2 characteristics. Rx can only observe the resultant frequency response caused by G_1, G_2 and H.

To overcome this issue, two practical PRC methods are proposed. The first one is the PRC with unified FDE (U-FDE) before BNLC. It is shown in Fig. 6. Comparing with Fig. 5(b), FDE2 in Fig. 5 is moved before BNLC and combined with FDE1. Rx simply measures the total frequency response and set the inverse transfer function in U-FDE. Thus, Rx need not separate G_1 and G_2. However, this configuration is not equivalent to the tandem FDE PRC because nonlinear compensation by BNLC is conducted after the equalization of G_1. This difference results in imperfect decomposition of linear distortion and nonlinear distortion and deteriorates equalization and nonlinear compensation performance. If the performance deterioration is within the acceptable level for practical applications, this method will be a good solution.

The other method is shown in Fig. 7. It introduces a Tx pre-equalizer to equalize the pre-filter G_1, instead of FDE2 at Rx. Owing to the pre-equalizer, the Wiener-Hammerstein memory effect is changed to the Hammerstein memory effect. Thus, the role of Rx FDE1 before BNLC is to equalize HG_2, which can be achieved independent of nonlinear distortion. The memory-effect characteristic of Tx can be measured and modeled when the Tx is prototyped. Therefore, we assume that the Tx pre-equalizer in Fig. 7 can be designed at the time of prototyping. Since SNR is high in Tx circuit, the pre-equalizer should have the inverse characteristic of G_1. Therefore, this method can provide good performance identical to the tandem FDE method whereas its feasibility is high.

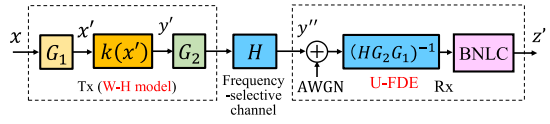

Fig. 6 PRC with U-FDE before BNLC.

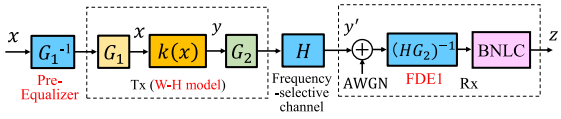

Fig. 7 PRC with FDE, BNLC and Tx pre-equalizer.

5. Performance Evaluation by Simulation

5.1 Simulation Condition and Settings

The performances of the proposed PRC schemes are evaluated through computer simulations in equivalent baseband using MATLAB. The transmitting signal is LTE-A/OFDM and modulation scheme is 64QAM. Performances are measured by the error vector magnitude (EVM) of the Rx output signal.

Table 1 lists the simulation conditions. Commonly used Saleh model [24] is employed as the memoryless nonlinear model. Since the third-order nonlinearity is dominant in the model, the maximum order of compensators is set to five. The sampling frequency is set 61.44 MHz to cover IM3 bandwidth (~27 MHz in baseband). The Tx memory effect is given by Wiener-Hammerstein model. The pre- and post-filters of the model are 2-tap Finite-Impulse Response (FIR) filters. The FIR tap interval is set 2 sample period (32.5 ns) and tap weights have complex (two-dimensional) Gauss distributions. No correlation is assumed between tap weights between pre- and post-filters. The maximum root mean square (RMS) delay spread created by a filter is 16.25 ns. It gives lowpass frequency response with cut-off frequency of around 10 MHz, which is close to the I/Q signal bandwidth of 9 MHz. The 3GPP-defined EPA channel model [6] is employed for frequency-selective channel model. Although EPA is a seven-tap FIR channel model with the maximum delay of 410 ns, power of the first to the fourth taps are dominant and the generated RMS delay spread is 47 ns. As a result, the delay spread caused by the Tx memory effect in the simulation is smaller than that caused by EPA model.

For the FDEs before BNLC in Rx, both ZF-FDE and MMSE-FDE are employed and evaluated. FDE2 in Fig. 5(b) and Tx pre-equalizer in Fig. 7 have the inverse transfer functions. In order to analyze the basic effect of FDE types on the PRC performance, it is assumed that FDEs perform ideally without equalizing error.

Table 1 Simulation settings.

Transmitting signal	LTE-A/OFDM
RF bandwidth	18.1 MHz
Modulation scheme	64QAM
Memoryless nonlinear model	Saleh model*
Tx output backoff	9 dB
Memory effect model	Wiener-Hammerstein
Pre- and post- memory effect filters	2-tap FIR
Frequency-selectivity fading model	EPA model (7 taps)
Max. nonlinear order of BNLC	5
Sampling frequency	61.44 MHz
Signal processing block size	4096 samples

$* \alpha_1 = 2,\ \beta_1 = 1,\ \alpha_2 = -\frac{\pi}{4},\ \beta_2 = -0.25$

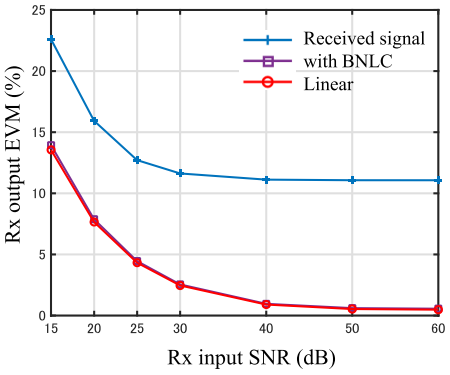

Fig. 8 EVM without fading and memory effect.

5.2 Basic Performance

Figure 8 shows the basic BNLC performance when Tx nonlinearity is memoryless and radio channel is flat without fading. For reference, Rx input EVM and EVM for linear transmission are added in blue and red colors, respectively. All EVM curves increases as the Rx input SNR decreases, which is due to AWGN. In the high SNR region, received signal EVM is around 12% that is caused by Tx nonlinearity. BNLC output EVM shown in purple color is reduced to less than 1%, very close to the linear transmission. Degradation of BNLC EVM from linear transmission is not obvious when the Rx input SNR is higher than 15 dB. It shows that BNLC is tolerant of AWGN in such SNR condition.

Next, we analyze the effect of Tx memory-effect on different PRC methods by observing frequency spectrum. Figure 9 shows examples of Rx output spectra for (a) BNLC alone, (b) tandem FDE and BNLC, (c) U-FDE and BNLC. All FDEs employ ZF algorism. The pre- and post-filters have peak gain at the lower edge of signal band and gain reduction of 3 dB at the upper edge. With BNLC alone in (a), nonlinear emission in adjacent bands is reduced by around 15 dB but deformation in signal spectrum cannot be equalized. With tandem FDE and BNLC in (b), spectrum equalization and nonlinear compensation are achieved in high levels. With U-FDE and BNLC in (c), the spectrum deformation can be equalized in the signal band and nonlinear distortion emission in adjacent bands is reduced by around 15 dB. The nonlinear compensation is not perfect as (b). Note that some part of outband spectra in high frequency region increase in (b) and (c). This is due to the noise enhancement effect of ZF-FDEs.

5.3 Performance in Frequency-Selective Fading

EVM performances for the proposed PRCs are evaluated in the presence of Tx memory effect and frequency-selective fading. Figure 10 shows relation of Rx input average SNR and output EVM. In the figure, (a) gives PRC performance with ZF-FDE, whereas (b) gives performance with MMSE-FDE. Compared with Fig. 8, EVM increase in low SNR region is faster due to the amplitude variation of fading for both (a) and (b). However, the increase of EVM in (a) is larger than in (b), regardless of conditions or PRC methods. This is due to the noise enhancement effect of ZF-FDE. The EVM difference between ZF and MMSE is around 10% for the SNR of 20 dB. It is concluded that MMSE-FDE is preferable for obtaining better EVM performance in the proposed PRC.

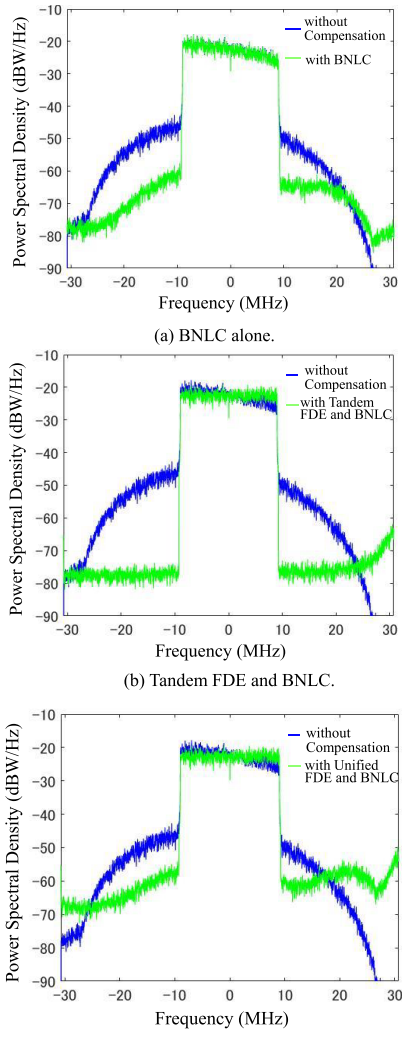

Fig. 9 Frequency spectra before and after PRC.

Focusing on the performance difference by PRC methods, PRC with FDE, BNLC and Tx pre-equalizer has the best EVM performances for both (a) and (b). The results are identical with that obtained by PRC with tandem FDE and BNLC. They are very close to the linear transmission case, which has been expected from the result of Fig. 9(b).

On the other hand, PRC with U-FDE before BNLC shown in red color in Fig. 10 presents higher EVM than the above PRCs by around 4% in the high SNR region. This degradation is doubled if the order of U-FDE and BNLC is inverted as shown in yellow color. EVM results in more than 10% even in the high SNR, which indicates that the PRC

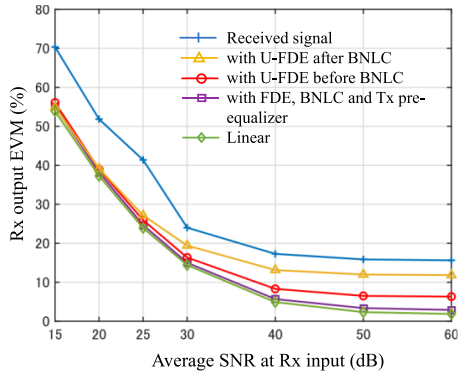

(a) ZF-FDE

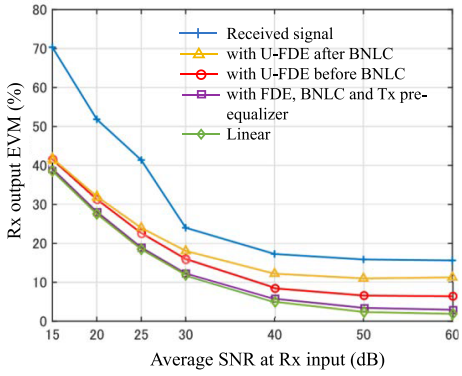

(b) MMSE-FDE

Fig. 10 Output EVM with fading and memory effect.

failed in accurate equalization and nonlinear compensation. When U-FDE is placed before BNLC, equalization of HG_2 can be perfect but equalization of G_1 is imperfect. This generates some error in the output signal. On the other hand, if U-FDE is placed after the BNLC, equalization of G_1 can be perfect but equalization of HG_2 is imperfect. Since the amount of linear distortion caused by HG_2 is greater than that by G_1, it will make the difference in output errors depending on the position of U-FDE. According to this reasoning, the difference will disappear if HG_2 is identical to G_1, for example, $H = 1$ and $G_1 = G_2$.

Figure 11 shows the effect of the fading channel impulse response length (CIRL) on the PRC performance at the average SNR of 60 dB. CIRL is varied by truncating longer FIR filter taps in the EPA model. CIRL of 0 ns means that only direct path exists and channel is characterized as flat Rayleigh fading channel. From the figure, Rx output EVM decreases as CIRL is shortened. The difference of EVMs depending on the U-FDE positions, before or after BNLC, is also reduced and disappear at null CIRL. Since the 2-taps FIR filters with the same tap interval and coefficient distributions are used for pre- and post-filters, the matching of EVMs at null CIRL is reasonable.

From above results, the proposed PRC with MMSE-FDE, BNLC and Tx pre-equalizer provides the best performance as a practical solution. EVM of less than 2.5% is achieved in high SNR region for 3GPP EPA channel, which enables the use of 256 QAM with 1% margin to 3GPP specification. This margin can be utilized to increase the output power or introduce the higher-level modulation such as 512 QAM with reasonable backoff in the future.

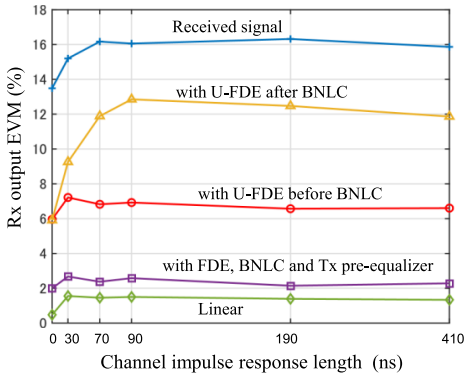

Fig. 11 CIRL vs. Output EVM at high SNR.

6. Conclusions

This paper studied BNLC-based post-reception nonlinear compensation (PRC) schemes that can compensate Tx memory nonlinearity through frequency-selective fading channel. We focused on the frequency-domain nonlinear modeling and proposed the compound distortion compensation method that separates linear equalization and nonlinear compensation by FDEs and BNLC. Tx memory effect and fading channel can be equalized by FDEs, whereas BNLC only compensates memoryless nonlinearity. Several PRC configurations were studied. Although the PRC with tandem FDE has ideal performance, it requires Tx memory model information at Rx side. Instead, practical PRC methods were proposed, PRC with unified FDE and BNLC, and PRC with FDE, BNLC and Tx pre-equalizer. Their performances were analyzed through computer simulations and evaluated by EVM. PRC performance in low SNR was also confirmed, in which MMSE-FDE provided better performance. By implementing the PRC in a base station, uplink performance will be enhanced without any additional cost and power consumption in user terminals.

References

[1] A. Dogra, R.K. Jha, and S. Jain, "A survey on beyond 5G network with the advent of 6G: Architecture and emerging technologies," IEEE Access, vol.9, pp.67512–67547, Oct. 2020.
[2] H. Elayan, O. Amin, R.M. Shubair, and M. Alouini, "Terahertz communication: The opportunities of wireless technology beyond 5G," Proc. Commet 2018, Marrakech, Morocco, April 2018.
[3] S.M.R. Islam, N. Avazov, O. Dobre, and K.S. Kwak, "Power-domain non-orthogonal multiple access (NOMA) in 5G systems: Potentials and challenges," IEEE Commun. Surveys Tuts., vol.19, no.2, pp.721–742, Second quarter 2017.
[4] J. Vuolevi and T. Rahkonen, Distortion in RF Power Amplifiers, Artech House, 2003.
[5] A.E. Saddic, "Digital twins: The convergence of multimedia technologies," IEEE Multimedia Mag, vol.25, no.2, pp.87–92, April–June 2018.
[6] 3GPP TS 36.101. version 14.5.0 Release 14, "Evolved Universal

Terrestrial Radio Access (E-UTRA); User Equipment (UE) Radio Transmission and Reception," 3rd Generation Partnership Project; Technical Specification Group Radio Access Network, pp.1332–1437, Nov. 2017.
[7] F.M. Ghannouchi and O. Hammi, "Behavioral modeling and predistortion," IEEE Microw. Mag., vol.10, no.7, pp.52–64, Dec. 2009.
[8] M. Valkama, A. Shahed, L. Anttila, and M. Renfors, "Advanced digital signal processing techniques for compensation of nonlinear distortion in wideband multicarrier radio receivers," IEEE Trans. Microw. Theory Techn., vol.54, no.6, pp.2356–2366, June 2006.
[9] K. Dogancay, "Blind compensation of nonlinear distortion for bandlimited signals," IEEE Trans. Circuits Syst. I, Reg. Papers, vol.52, no.9, pp.1872–1882, Sept. 2005.
[10] Y. Ma and Y. Yamao, "Blind nonlinear compensation technique for RF receiver front-end," Proc. 43rd European Microwave Conf., pp.1527–1530, Nuremberg, Germany, Oct. 2013.
[11] Y. Ma, Y. Yamao, K. Ishibashi, and Y. Akaiwa, "Adaptive compensation of inter-band modulation distortion for tunable concurrent dual-band receivers," IEEE Trans. Microw. Theory Techn., vol.61, no.12, pp.4209–4219, Dec. 2013.
[12] K. Kimura and Y. Yamao, "Bandwidth-efficient blind nonlinear compensation of RF receiver employing folded-spectrum sub-nyquist sampling technique," IEICE Trans. Commun., vol.E102-B, no.3, pp.632–640, March 2019.
[13] T. Abe and Y. Yamao, "Blind post-compensation of tandem nonlinearly caused by transmitter and receiver," Proc. IEEE RWS2020, pp.12–15, San Antonio, USA, Jan. 2020.
[14] J. Nagai, K. Ishibashi, and Y. Yamao, "Signal quality improvement in downlink power domain NOMA with blind nonlinear compensator and frequency domain equalizer," IEICE Trans. Commun., vol.E105-B, no.5, pp.648–656, May 2022.
[15] H. Ito, T. Fujii, and Y. Yamao, "Post-reception compensation performance of blind nonlinear compensator with equalizer against memory nonlinear distortion," Proc. IEEE VTC2020-Fall, Nov. 2020.
[16] L. Ding, G.T. Zhou, D.R. Morgan, Z. Ma, J.S. Kenney, J. Kim, and C.R. Giardina, "A robust digital baseband predistorter constructed using memory polynomials," IEEE Trans. Commun., vol.52, no.1, pp.159–165, Jan. 2004.
[17] D.R. Morgan, Z. Ma, J. Kim, M.G. Zierdt, and J. Pastalan, "A generalized memory polynomial model for digital predistortion of RF power amplifiers," IEEE Trans. Signal Process., vol.54, no.10, pp.3852–3860, Sept. 2006.
[18] L. Sung, Y. Ding, and A. Sano, "Identification-based predistortion scheme for high power amplifiers," IEICE Trans. Fundamentals, vol.E86-A, no.4, pp.874–881, April 2003.
[19] J.C. Pedro and S.A. Maas, "A comparative overview of microwave and wireless power-amplifier behavioral modeling approaches," IEEE Trans. Microw. Theory Techn., vol.53, no.4, pp.1150–1163, April 2005.
[20] R. Raich, H. Qian, and G.T. Zhou, "Orthogonal polynomials for power amplifier modeling and predistorter design," Proc. IEEE Trans. Veh. Technol., vol.53, no.5, pp.1468–1479, Sept. 2004.
[21] H. Sari, G. Karam, and I. Jeanclaude, "Frequency-domain equalization of mobile radio and terrestrial broadcast channels," Proc. GLOBECOM'94, San Francisco, CA, Nov. 1994.
[22] M.V. Clark, "Adaptive frequency-domain equalization and diversity combining for broadband wireless communications," IEEE J. Sele. Areas Commun., vol.16, no.8, pp.1385–1395, Oct. 1998.
[23] D. Falconer, S.L. Ariyavisitakul, A. Benyamin-Seeyar, and B. Eidson, "Frequency domain equalization for single-carrier broadband wireless systems," IEEE Commun. Mag., vol.40, no.4, pp.58–67, April 2002.
[24] A.M. Saleh, "Frequency-independent and frequency-dependent nonlinear models of TWT amplifiers," IEEE Trans. Commun., vol.29, no.11, pp.1715–1720, Nov. 1981.

Yasushi Yamao received his B.S., M.S., and Ph.D. degrees in electronics engineering from Kyoto University, Kyoto, Japan, in 1977, 1979, and 1998, respectively. He began his research career in mobile communications in the measurement and analysis of urban radio propagation as his M.S. thesis. In 1979, he joined the Nippon Telegraph and Telephone Corporation (NTT) Laboratories, Japan, where his major activities included leading research on GMSK modulator/demodulator and GaAs RF ICs for digital mobile communications, and development of PDC digital cellular handheld phones. In 1993, he moved to NTT DoCoMo Inc. and directed the standardization of a high-speed paging system (FLEX-TD) and the development of a 3G radio network system. He also joined the European IST research programs for IP-based 4th generation mobile communication. In 2005, he moved to the University of Electro-Communications as a professor of the Advanced Wireless Communication Research Center (AWCC). His interests include wireless communication networks and protocols, as well as high-efficiency and reconfigurable wireless circuit technologies in both RF and Digital Signal Processing. Prof. Yamao is a Fellow of the IEICE, member of IPSJ and life member of the IEEE. He has served as the Vice President of IEICE Communications Society (2003–2004), the Chairman of IEICE Technical Group on Radio Communication Systems (2006–2008), the Chief Editor of IEICE Communication Magazine (2008–2010), the Vice Chairman of IEEE VTS Japan chapter (2009–2015), a Director of the IEICE (2015–2017), and the Chairman of IEEE VTS Japan chapter (2019–2021).

Tetsuki Taniguchi received the B.S. and M.S. degrees in electrical engineering from Tokyo Metropolitan University in 1989 and 1991. In 1992, he joined Kanazawa University, where he worked as a research assistant and a researcher, and received D.E. degree in 1996. In 2001, he moved to the University of Electro-Communications (UEC), then started working at Tokyo Institute of technology in 2016. Since 2019, he is a researcher at the advanced wireless and communication research center (AWCC), UEC. His research interests are digital signal processing and propagation analysis in digital communications.

Hiroki Ito received his B.S. and M.S. degrees in Electrical Engineering from the University of Electro-Communications in 2020 and 2022, respectively. He is now working with NTT DoCoMo Inc.